Geophysical Research Letters

RESEARCH LETTER
10.1029/2023GL106367

Deep Atlantic Multidecadal Variability

Jiajun Yang[1], Jianping Li[1,2], and Qirong An[1,2]

[1]Frontiers Science Center for Deep Ocean Multi-spheres and Earth System (DOMES)/Key Laboratory of Physical Oceanography/Academy of Future Ocean/College of Oceanic and Atmospheric Sciences, Ocean University of China, Qingdao, China, [2]Laoshan Laboratory, Qingdao, China

Key Points:

- Deep Atlantic Multidecadal Variability (DAMV) displays a mid-high latitudes north-south dipole pattern with a quasi-period of 20–50 years
- The meridional ocean heat transport, driven by the Atlantic Meridional Overturning Circulation (AMOC), can explain the DAMV variation
- The AMOC transports surface heat downwards over more than a decade and contributes to the DAMV pattern in the deep Atlantic

Supporting Information:

Supporting Information may be found in the online version of this article.

Correspondence to:

J. Li,
ljp@ouc.edu.cn

Citation:

Yang, J., Li, J., & An, Q. (2024). Deep Atlantic multidecadal variability. *Geophysical Research Letters*, *51*, e2023GL106367. https://doi.org/10.1029/2023GL106367

Received 29 SEP 2023
Accepted 21 DEC 2023

Author Contributions:

Conceptualization: Jianping Li
Formal analysis: Jiajun Yang, Jianping Li, Qirong An
Funding acquisition: Jianping Li
Investigation: Jiajun Yang, Jianping Li
Methodology: Jiajun Yang, Jianping Li, Qirong An
Project Administration: Jianping Li
Software: Jiajun Yang
Supervision: Jianping Li, Qirong An
Validation: Jiajun Yang
Visualization: Jiajun Yang
Writing – original draft: Jiajun Yang
Writing – review & editing: Jiajun Yang, Jianping Li, Qirong An

Abstract Investigating deep-sea temperature variability is essential for understanding deep-sea variability and its profound impacts on climate. The first mode in the Atlantic is referred to as Deep Atlantic Multidecadal Variability (DAMV), characterized by a north-south dipole pattern in the mid-high latitudes with a quasi-period of 20–50 years. The DAMV and Atlantic Multidecadal Variability, despite a statistical discrepancy, may be different responses to ocean heat transport (OHT) driven by the Atlantic Meridional Overturning Circulation (AMOC) at distinct depths separately. The relationship between the DAMV and the AMOC is established, indicating the AMOC is likely to transport surface heat downwards by deep convection and contribute to such dipole pattern in the deep Atlantic. Furthermore, meridional OHT proves the AMOC can explain the DAMV variation as a dynamic driver. These results reinforce the importance of deep-sea studies concerning the Atlantic climate system.

Plain Language Summary The deep sea is an indispensable component of the Earth's climate system, owing to its substantial heat capacity. Despite challenges posed by the reliability of ocean data sets deeper than 2,000 m, exploration of the deep sea is of immense social and scientific significance. This study identifies the dominant mode of deep Atlantic potential temperature at a depth of approximately 3,000 m, known as Deep Atlantic Multidecadal Variability (DAMV). The DAMV exhibits a dipole pattern in the mid-high latitudes, cooling (warming) in the North Atlantic and warming (cooling) in the South Atlantic during its positive (negative) phase. The DAMV is a multidecadal variability with a meaningful quasi-period of 20–50 years, similar to the Atlantic Multidecadal Variability (AMV). However, statistical methods indicate that the DAMV and the AMV are distinct climate variabilities, closely connected by the AMOC. By lead-lag correlation and ocean heat transport analysis, deep convection of the AMOC might facilitate the surface heat downward transport over approximately a decade. As a result, it is highly likely that the DAMV pattern can be attributed to the AMOC.

1. Introduction

The ocean, a pivotal component of the Earth's system, assumes an irreplaceable role in the regulation of global warming, especially the deep sea (Chen & Tung, 2014; Trenberth et al., 2016). A multitude of studies identify the dominant modes of sea surface temperature (SST) in the Atlantic basin. Additionally, several articles delve into Atlantic subsurface temperature, uncovering their profound impacts on climate, socioeconomics, and human well-being, which are of great research value.

The dominant mode of SST, known as the Atlantic Multidecadal Oscillation, reveals a dipole pattern spanning the entire Atlantic basin with a quasi-period of 50–80 years. It is brought to the forefront for its significant impacts on Atlantic hurricanes, African Sahel rainfall, and summer climate of North America (Enfield et al., 2001; Goldenberg et al., 2001; Kerr, 2000; McCabe et al., 2004; Rowell, 2003). Recent research suggests it is more appropriate to be referred to as Atlantic Multidecadal Variability (AMV) due to its broader band of low-frequency signals (Sutton et al., 2018; Zhang et al., 2019). The AMV is linked to the oceanic thermohaline circulation, which is fundamental in reconstructing past thermohaline circulation (Delworth & Mann, 2000; Knight et al., 2005). Additionally, some studies indicate an inter-hemispheric asymmetric mode of global SST with a spatial pattern in the Atlantic closely resembling the AMV (Dima & Lohmann, 2010), referred to as the SST inter-hemispheric dipole mode in subsequent research. Previous studies affirm its distinction from the AMV and its contribution to the asymmetry of tropical rainfall (Sun et al., 2013). As for the interannual timescale, the North Atlantic SST triple pattern is worthy of further investigation, as it influences spring Eurasian wildfire, early spring atmospheric circulation, and more (Han et al., 2016; Meng & Gong, 2022).

Numerous studies discuss the dominant mode of Atlantic subsurface temperature and endeavor to elucidate the underlying physical mechanisms. By utilizing both instrumental and model-simulated subsurface potential temperature data at a depth of 400 m, the dominant mode manifests a dipole pattern in the North Atlantic. It can be regarded as a fingerprint of the Atlantic Meridional Overturning Circulation (AMOC), consequently enhancing the predictability of the AMOC variability (Zhang, 2008).

Investigating the dominant mode of the deep Atlantic at depths exceeding 1,000 m, represents a significant stride in deep-sea science, which in turn contributes to advancements in aquaculture, bioscience, energy resources and other domains. However, only a limited number of studies focus on deep-sea variability, due to constraints from observation capability and climate model bias.

The EN data set version 4 (EN4) offers promising avenues for discovering deep sea and is extensively employed in various deep-sea studies. Notably, there is a consistency about the trend of ocean heat content in the Atlantic upper 700 m across four data sets, including the EN4 data set (Liu et al., 2016). Concerning ocean heat content within the 700−2,000 m and its trend, the EN4 has feasibility (Trenberth et al., 2016). To discuss reversal of climate trends in the North Atlantic, previous research uses the EN4 to calculate ocean potential density (Robson et al., 2016). And taking advantage of the EN4 to calculate thickness of the Labrador Sea Water proves rational for quantifying freshwater flux in deep water formation (Yang et al., 2016). Thus, the EN4 data set is chosen to investigate the dominant mode of deep Atlantic potential temperature variability.

2. Data and Methods

This paper makes use of deep sea potential temperature (DSPT) from the EN data set version 4.2.2 at 1° × 1° longitude/latitude grid resolution. In order to be constrained by observations, the EN4 data set assimilates a variety of temperature and salinity observation data from the Arctic Synoptic Basin Wide Oceanography project, the Global Temperature and Salinity Profile program, and the Array for Real-time Geostrophic Oceanography project (Good et al., 2013). Acknowledging a key limitation of the EN4 data set, which relaxes to climatology in data-sparse regions, a threshold value method involving the standard deviation of a moving 19-year series is applied. The effective grid proportion in the Atlantic basin has reached up to 90% since 1950, indicating original DSPT data is effective to explore the dominant modes (Figure S1 in Supporting Information S1). Due to tiny month-to-month DSPT variations, annual mean DSPT data from 1950 to 2021 is used.

Furthermore, the state-of-the-art deep-sea observing programs, the Overturning in the Subpolar North Atlantic Program (OSNAP) and the South Atlantic Meridional Overturning Circulation (SAMOC) observing systems which are highly unlikely to be assimilated into the EN4 data set (Discussed with the EN4 data set principals and reconfirmed), are employed. By the Haversine formula, a comparison is drawn between the gridded observational DSPT time series from 2014 to 2018 and the closest EN4 gridded time series. On the one hand, the average relative error at each grid point is 4.64% for the OSNAP and 5.31% for the SAMOC. Regarding the root mean square error, the OSNAP records 0.095 and the SAMOC is 0.096. These indicate that DSPT deviations between the EN4 data set and the observing programs are acceptable. On the other hand, the average correlation coefficient for the OSNAP is 0.80 and for the SAMOC is 0.52, indicating two types of DSPT data are highly matched. Overall, the EN4 data set can be used to investigate the deep Atlantic.

To draw a robust conclusion grounded in both observations and modeling, the Coupled Model Intercomparison Project Phase 6 (CMIP6) model outputs and Australian Community Climate and Earth System Simulator Ocean Model version 2 (ACCESS-OM2) is introduced. Among comparable models, the ACCESS-OM2 stands out due to its accurate representation of large-scale overturning circulation and patterns of western boundary currents realistically (Kiss et al., 2020; Li et al., 2023). The SST data are extracted from the Extended Reconstruction Sea Surface Temperature (ERSST) data set version 5, the Hadley Center Sea Ice and Sea Surface Temperature (HadISST) data set version 1, and the Berkeley Earth Monthly Land and Ocean Surface Temperature (BEST) data set. To show the strike of the Mid-Atlantic Ridge, the ETOPO1 global relief model is applied here.

The empirical orthogonal function (EOF) analysis is performed on the annual mean DSPT in the Atlantic after removal of a linear fit to the global mean. The power spectrum is applied to quantify the temporal behavior of DSPT variability. Given the focus on decadal to multidecadal variability in the deep sea, a 9-year Gauss lowpass filter is applied. The SST-based AMOC index is defined as the difference between two key regions of the AMV situated between 40°−60°N, 60°−10°W and 40°−60°S, 50°W−0° (Keenlyside et al., 2008; Latif et al., 2006).

And the AMOC stream function index is defined as the maximum overturning stream function at a special latitude (typically 30°N):

$$\psi(y,z) = \int_{X_{\text{west}}}^{X_{\text{east}}} \mathrm{dx} \int_{z}^{\eta} v(x,y,z)dz \tag{1}$$

where v is the meridional velocity; X_{east} and X_{west} are the eastern and western boundary; z is the ocean depth; and η is the free surface height. Meridional ocean heat transport (OHT) is calculated within a certain layer:

$$\mathrm{OHT}(y) = \int_{X_{\text{west}}}^{X_{\text{east}}} \int_{-H_1}^{-H_2} \rho_0 C_p v(x,y,z)\theta(x,y,z)\mathrm{dzdx} \tag{2}$$

where C_p is the constant specific heat capacity (3,991 J•kg^{-1} • K^{-1}); ρ_0 is sea water density; H_1 and H_2 are the lower and upper limit of the certain layer; θ is potential temperature; and v is meridional velocity. Note that all the significances of the correlation coefficients are accessed on the basis of the effective number of degrees of freedom, in consideration of autocorrelation between two individual time series (Davis, 1978; Li et al., 2012):

$$\frac{1}{N^{\text{eff}}} \approx \frac{1}{N} + \frac{2}{N}\sum_{j=1}^{N}\frac{N-j}{N}\rho_{xx}(j)\rho_{yy}(j) \tag{3}$$

where N^{eff} is the effective number of degrees of freedom; N is sample size; $\rho_{xx}(j)$ and $\rho_{yy}(j)$ are autocorrelations of time series X and Y at time lag j.

3. Deep Atlantic Multidecadal Variability

Deep sea typically refers to ocean depths greater than 1,000 m (Hayes et al., 2021; Mat et al., 2020), thereby concentrating research efforts on a certain layer of the deep Atlantic for simplified investigations. Referred to the vertical profile of northward transport in Atlantic basin, the boundary between upper North Atlantic Deep Water (NADW) and lower NADW is delineated around 3,000 m (Cunningham et al., 2007). Hence, the EOF method is applied to the 3,269 m DSPT. According to the rule of thumb, significance of dominant modes derived from the EOF method can be evaluated statistically (North et al., 1982). The first mode, referred to as Deep Atlantic Multidecadal Variability (DAMV), is distinguished clearly from the rest of eigenvectors (Figure S3 in Supporting Information S1). And the explained variance of the DAMV is 31.31%, surpassing that of the second mode by threefold. Consequently, this study pays more attention to the first mode DAMV.

The DAMV features a prominent north-south dipole pattern in the mid-high latitudes of the Atlantic basin as Figure 1a depicts. This pattern features two pronounced loading centers indicated by the black boxes: the north key region box (45°−60°N, 50°−35°W) and the south key region box (25°−40°S, 50°−35°W). These key regions are relatively close to the western boundary. Notably, the two prominent loading regions are relatively close to the western boundary, while the signal extends toward the Mid-Atlantic Ridge shown as a dashed line, which may be associated with the formation and mixture of Antarctic Bottom Water (Rintoul, 1991). Moreover, previous studies display that the NADW sinks into deep ocean around 3,000 m in the latitudes between 40°N and 60°N, and rises in the latitudes around 30°–50°S matching the latitudes range of DAMV (Marshall & Speer, 2012; McCarthy et al., 2020). Hence, we surmise physical interpretation of two DAMV key regions might be associated with the NADW which needs further research. During the positive (negative) phase of the DAMV, the mid-high latitudes of the South Atlantic is dominated by a warming (cooling) signal, while the mid-high latitudes of the North Atlantic appears to be cooling (warming). Figure 1c suggests the principal component corresponding to the DAMV (PC1) is dominated by multidecadal variability, marked by a solitary decadal transition from negative phase to positive phase around 1980−1990. According to the power spectrum shown in Figure 1d, the DAMV displays a wide range of meaningful quasi-period of 20–50 years, with a low-frequency peak at approximately 50 years. And quasi-periodicity of the DAMV is likely to extend a broader range, potentially limited by the time span of the EN4 data set.

A previous study uses observation station data from World Data Center-B and finds a significant warming trend in the North Atlantic at depths from 800 to 2,500 m during the period 1957−1981 (Antonov, 1993). It aligns with the warming signal observed in the mid-high latitudes of the North Atlantic during the negative phase of the DAMV, promoting the robustness of the DAMV in some way.

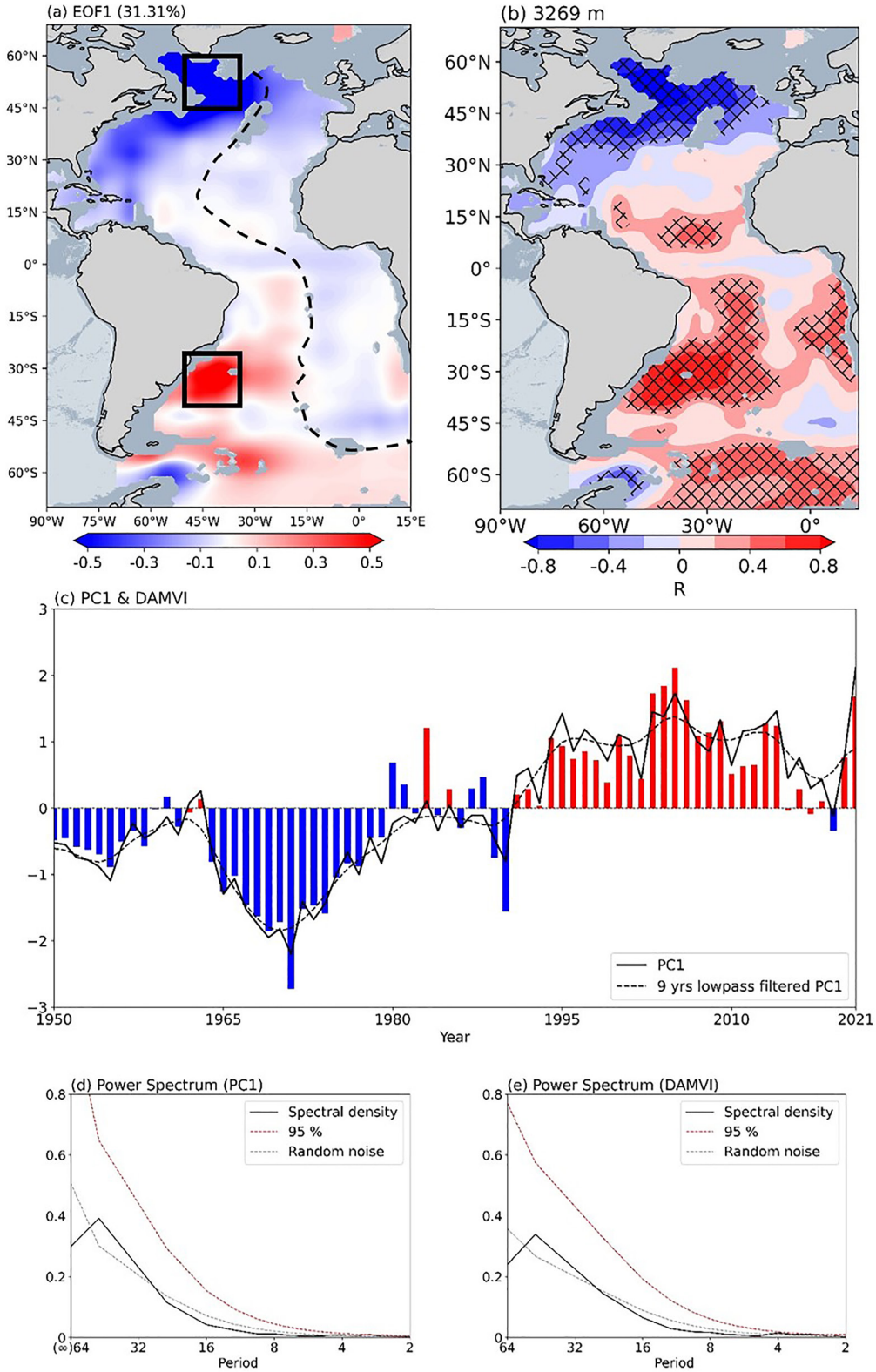

Figure 1.

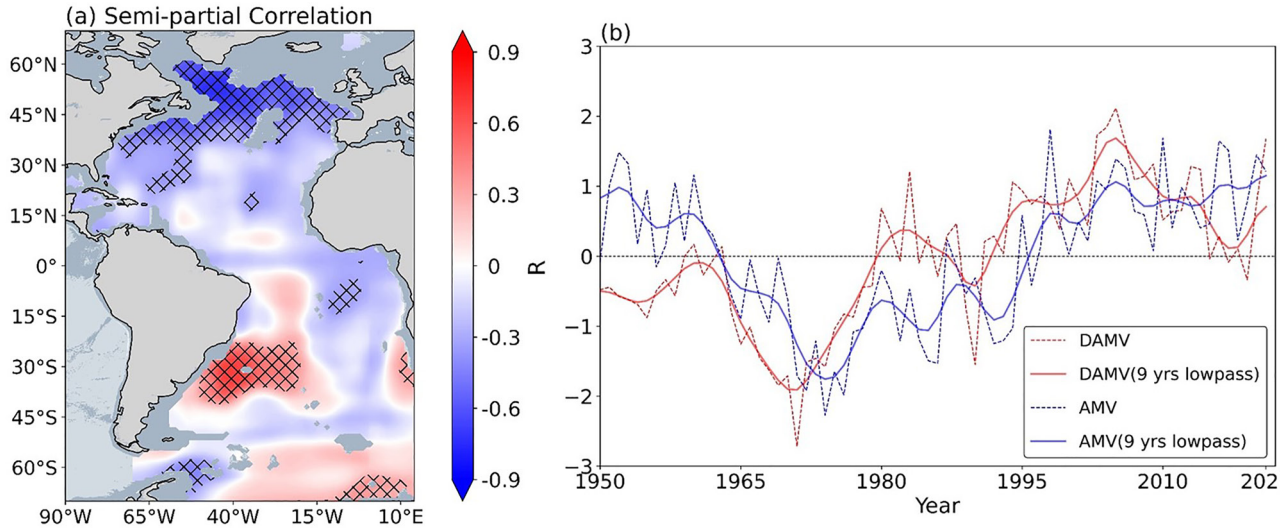

Figure 2. (a) The correlation map between the Deep Atlantic Multidecadal Variability index (DAMVI) and residual deep sea potential temperature (70°S−70°N) over the period 1950−2021 with the Atlantic Multidecadal Variability (AMV) signal linearly removed, and the areas marked by crosses are significant at the 95% confidence level. Continents are masked in taupe, submarine topography less than 3,269 m deep is masked in gray, and that more than 3,269 m deep is masked in dark gray. (b) Standardized annual mean time series (1950−2021) of the DAMVI (dashed red line), the AMV index (dashed blue line), the 9-year lowpass filtered DAMVI (solid red line), and 9-year lowpass filtered AMV index (solid blue line).

For ease of calculation, the DAMV index (DAMVI) is defined as the detrended DSPT anomaly averaged over the south key region (25°−40°S, 50°−35°W) subtracted from that over the north key region (45°−60°N, 50°−35°W). Figure 1c demonstrates the DAMVI is highly correlated with the PC1, with a correlation coefficient of 0.95 statistically significant at the 99% confidence level, suggesting the proposed DAMVI serves as an appropriate indicator of the DAMV. To evaluate whether the DAMVI can capture the primary spatio-temporal characteristics, both correlation analysis and power spectrum are applied. Figure 1b illustrates the correlation map between the DAMVI and DSPT anomaly, revealing a DAMV-like pattern. Focusing on the DAMV key regions, the area-averaged correlation coefficient is 0.68 for the south region and −0.83 for the north one, suggesting the DAMVI is well-matched in spatial pattern. Figure 1e shows power spectrum of the DAMVI highlighting a meaningful quasi-periodic character spanning approximately 20–50 years. In summary, the proposed DAMVI successfully catch the primary characteristics of the DAMV in both spatial and temporal domains, suggesting its suitability as an indicator for further research. Moreover, the DAMVI effectively quantifies opposing changes in deep Atlantic mid-high latitudes potential temperature, with an explained variance reaching up to 90.25%, underscoring that the DAMVI has a clearer physical interpretation compared to the PC1.

The DAMV and the AMV, serving as the dominant mode of Atlantic DSPT and SST respectively, have similar spatio-temporal characteristics. Both of them exhibiting a dipole pattern are dominated by multidecadal variability. However, it is crucial to underscore that despite these similarities, the DAMV and AMV are two distinct climate variabilities obviously due to their differing depths. In terms of spatial pattern, the AMV exhibits a dipole pattern over the entire Atlantic basin instead of only in mid-high latitudes where the DAMV exhibits. Their differences in temporal evolution are still obvious qualitatively. The decadal transition of the DAMV occurs around 1980, leading that of the AMV a decade presumably. According to power spectrum, the AMV shows a broad significant band at the multidecadal time scale 50−80 years differing from the DAMV (Gulev et al., 2013; Tung & Zhou, 2013).

To quantify the differences between the DAMV and the AMV, semi-partial correlation is introduced to remove partial influence of the AMV on the DSPT. Figure 2a further displays the correlation map between the DAMVI

Figure 1. Spatio-temporal characteristics of the Deep Atlantic Multidecadal Variability (DAMV). (a) Spatial pattern of the DAMV. The two black boxes indicate key regions of the DAMV: the northern box (45°–60°N, 50°–35°W) and the southern box (25°–40°S, 50°–35°W). Dashed line indicates the strike of the Mid-Atlantic Ridge. (b) The correlation map between the DAMV index and the deep sea potential temperature anomaly (1950–2021), and the areas marked by crosses are significant at the 95% confidence level. Continents are masked in taupe, submarine topography more than 3,269 m deep is masked in gray and that less than 3,269 m deep is in dark gray. (c) Standardized annual mean time series (1950–2021) of the DAMV index (bar), the principal component corresponding to the DAMV (PC1) (solid black) and its 9-year lowpass filtered series (dashed black). (d) Power spectrum of the PC1 (red line is the 95% significance level corresponding to the red noise spectrum and gray line is red noise line). (e) The same as (d), but for the DAMV index.

and residual DSPT anomaly over 1950−2021 after linear removal of the AMV signal (subtracting the regression onto the AMV index). The robust north-south dipole pattern in the mid-high latitudes is still evident, highly similar to the DAMV pattern. Figure 2b shows the DAMVI is correlated with the AMV index ($r = 0.51$ for annual mean series, $r = 0.60$ for 9-year lowpass filtered series), suggesting there is an association between two variabilities at decadal timescale in spite of above-discussed differences. Moreover, the DAMV seemingly leads the AMV by approximately a decade, hinting at their objective similarity which needs for further investigation.

4. Relationship Between the DAMV and the AMOC

Many studies reveal both directly observed AMOC variability and its fingerprint are closely linked to the AMV signal, implying the DAMV might relate to the AMOC (Frajka-Williams et al., 2016; Smeed et al., 2018; Yan et al., 2017). And referred to the similarity between the DAMV and the AMV, we surmise they might be interconnected by the AMOC acting as a dynamic driver, considered as different responses to OHT driven by the AMOC in DSPT and SST separately.

To validate the aforementioned surmise, Figure 3a shows the lead-lag correlation map between the DAMVI and the AMOC stream function index on a decadal timescale. On one hand, the AMOC lags the DAMV by nearly 6−22 years. And prominent lag correlation coefficient is 0.76 when the AMOC lags the DAMV by 16 years. It underscores the substantial value of investigating the DAMV, particularly concerning the AMOC. Providing a new perspective from the deep Atlantic is likely to improve our comprehension and potentially prediction of the AMOC variation. On the other hand, the negative AMOC leads the DAMV by around 8−17 years. A notable negative peak emerges with a lead of approximately 13 years (AMOC leading DAMV) with the lead correlation coefficient reaching −0.62. Previous research indicates that deep convection induced by overturning is an essential component of the AMOC, and timescale of deep convection in the subpolar North Atlantic is on the order of a decade aligned with the lead relationship (Ba et al., 2013; Winton & Sarachik, 1993). It takes a decade approximately to transport the surface ocean heat downward by deep convection of the AMOC, further supporting the rationality of the relationship in timescale. As for spatial scale, Figure 3b shows the correlation map as the AMOC leading DSPT by 13 years, there is an obvious north-south dipole pattern in the mid-high latitudes. It indicates the response of the AMOC to DSPT contains a DAMV-like pattern when the AMOC leads by 13 years, possibly contributing to formation of the north-south dipole pattern in mid-high latitudes. Hence, the AMOC may have association with the DAMV, both in timescale and in spatial pattern presumably. In addition, the SST-based AMOC index is applied to draw a robust conclusion about the relationship between the DAMV and the AMOC. The response of the AMOC to DSPT still shows a DAMV-like pattern when the AMOC leading by approximately two decades, implying a robust relationship between the DAMV and the AMOC.

Furthermore, the meridional OHT analysis is employed to shed light on the physical processes about AMOC and DAMV relationship. Figure 3c shows net meridional OHT changes in two key regions of the DAMV in the period 1958−2021 based on the ACCESS-OM2 model. In these key regions, net meridional OHT is defined as the meridional OHT at the northern boundary minus that at the southern boundary. The blue line denoting the north key region exhibits negative in the former part, while shifts to be positive in the latter part. The transition occurs around 1980 to 1990, coinciding with phase transition of the DAMV. During negative phase of the DAMV, the northern boundary of the north key region illustrates a southward heat transport in comparison to the southern boundary. It indicates that more heat is stored within the north key region, leading to a rise of DSPT in the north key region in the DAMV negative phase. Conversely, the northern boundary shows a northward OHT during the DAMV positive phase. It points out that poleward OHT plays a leading role in the north key region during the DAMV positive phase. As more heat is transported out of the north key region, DSPT decreases during the DAMV positive phase. It is highly consistent with spatio-temporal characteristics of the DAMV. As for the south key region shown in red, it is positive from 1958 to 1980 or so, and then turns to be negative concurrent with the DAMV phase transition as well. During negative (positive) phase of the DAMV, the northern boundary of the south key region experiences a northward (southward) heat transport. This reveals that the south key region stores less (more) heat, leading to DSPT decreases (rises) synchronously. In a word, the meridional OHT, driven by the AMOC, effectively explains the contrasting changes of deep Atlantic potential temperature in mid-high latitudes.

5. Conclusions and Discussion

Based on the EN4 data set, the dominant mode of DSPT in the Atlantic is investigated and referred to as the DAMV, which is separated statistically and of great research value. The DAMV is characterized by a pronounced

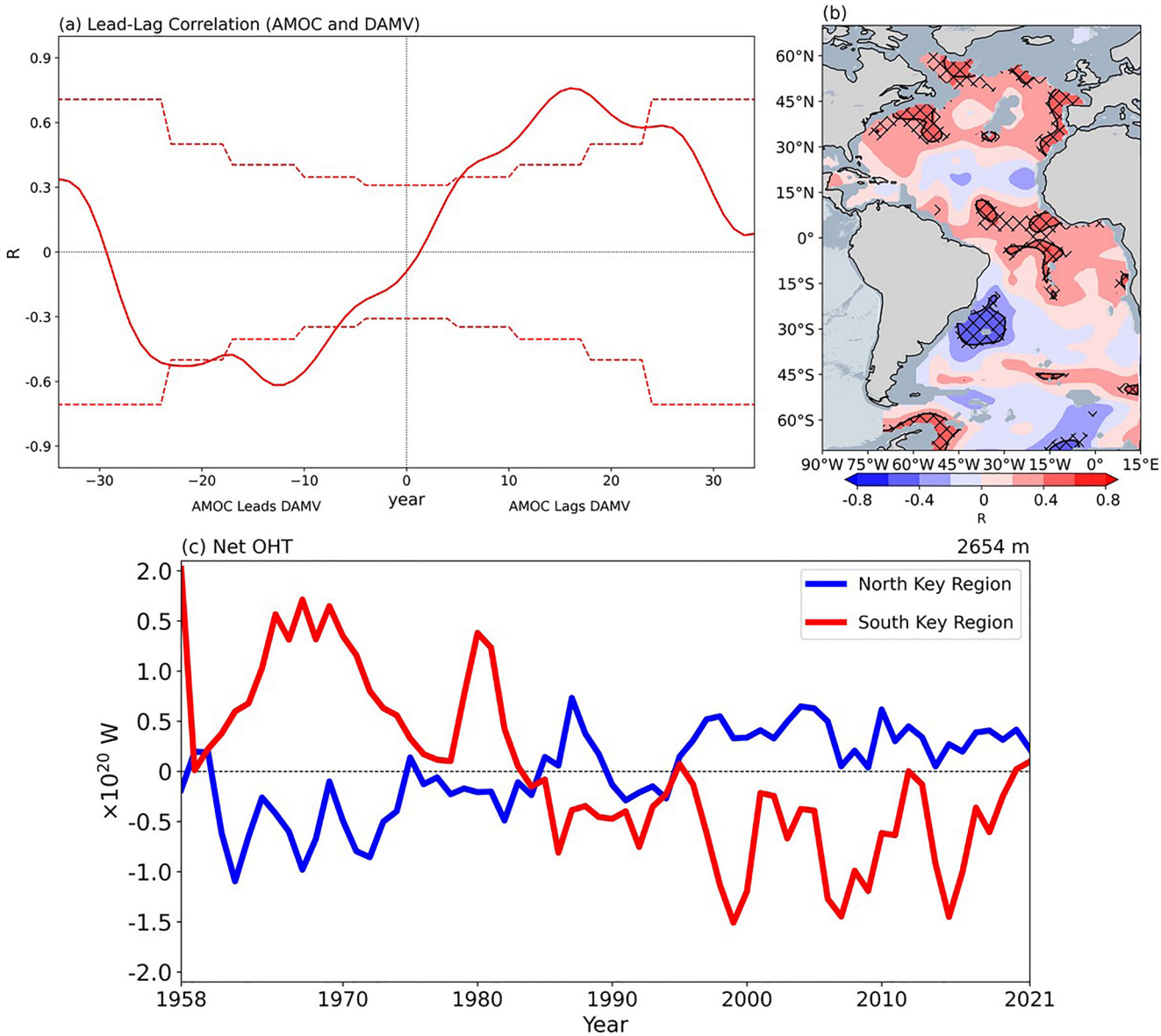

Figure 3. Relationship between the Deep Atlantic Multidecadal Variability (DAMV) and the Atlantic Meridional Overturning Circulation (AMOC). (a) Lead-lag correlation between the 9-year lowpass filtered DAMV index and 9-year lowpass filtered AMOC stream function index, and the dashed line denote the 95% confidence levels using the effective number of degrees of freedom. (b) The lead correlation map about the AMOC stream function index leading the deep sea potential temperature anomaly 13 years. The areas marked by crosses are significant at the 90% confidence level and the black solid line denote the areas are significant at the 95% confidence level. Continents are masked in taupe, submarine topography more than 3,269 m deep is masked in gray, and that less than 3,269 m deep is masked in dark gray. (c) Time series (1958−2021) of net meridional ocean heat transport in two key regions of the DAMV in the Australian Community Climate and Earth System Simulator Ocean Model version 2 (north key region in blue and south key region in red).

north-south dipole pattern in the mid-high latitudes of the Atlantic basin, with a wide range of quasi-period 20−50 years approximately. And the proposed DAMVI is a proper indicator of the DAMV both in temporal and in spatial. High correlation relationship between the PC1 and the DAMVI confirms the DAMV can represent the opposing DSPT changing within the mid-high latitudes of the deep Atlantic. To enhance the robustness of DAMV, we introduce the ACCESS-OM2 model to find the DAMV at a depth of 2,654 m successfully, which displays a significant quasi-period from 20 to 60 years at a 95% significance level (Figure S4 in Supporting Information S1). It is shallower in the model compared to observations which could potentially be attributed to the shallower mean AMOC in this model (Hirschi et al., 2020). Moreover, the DAMV is identified in the two pre-industrial control simulation from the CMIP6: CESM2 (1,200 years) and GFDL-ESM4 (500 years),

providing two more model evidence to clarify that the DAMV is a robust deep Atlantic potential temperature variability (Figure S5 in Supporting Information S1).

The DAMV and the AMV indeed exhibit a close statistical association, yet remain distinct climate variabilities due to obvious different depths. This relationship ought to be ascribed to the AMOC as the responses to two distinct characteristic depths in the Atlantic, and it will be a meaningful and interesting research which needs further research to unveil mystery of deep Atlantic. And Figure S6 in Supporting Information S1 reveals that the response of the DAMV to SST exhibits a robust warming-hole-like pattern that is associated with decline of the AMOC probably (Drijfhout et al., 2012), implying the DAMV may be affected by the AMOC. On one hand, lead correlation coefficient of −0.62 (AMOC leading DAMV by 13 years), aligns with the timescale of deep convection. On the other hand, the response of the AMOC to DSPT when AMOC leading by 13 years contains the DAMV signal. Moreover, net meridional OHT in two DAMV key regions well-match spatio-temporal features of the DAMV. Therefore, the AMOC acts as a dynamic driver in variation and evolution of the DAMV with high probability. And the DAMV is likely to be the key for understanding the processes of deep Atlantic heat transport driven by the AMOC, which needs more sustained in-situ deep sea observation systems to get deep sea velocity field with high accuracy.

At last, there are two possible uncertainties for this study. (a) The observation-only data set of deep Atlantic potential temperature is shorter and scarcer compared with SST data sets. Hence, the uncertainty of deep sea data set used in this study remains indeed. (b) The robustness of the DAMV deserves to be enhanced by more model-simulated data sets with longer time span improving the robustness of our conclusions, which deserves further investigation.

Data Availability Statement

Deep sea potential temperature data from the EN data set version 4.2.2 is available online at https://www.metoffice.gov.uk/hadobs/en4/download-en4-2-2.html (Good et al., 2013). The ACCESS-OM2 model data (Kiss et al., 2020) is from https://dapds00.nci.org.au/thredds/catalogs/cj50/access-om2/cf-compliant/cf-compliant.html. The CMIP6 model outputs used in this study may be downloaded freely at https://esgf-node.llnl.gov/projects/cmip6/. The observation data from 2014 to 2018 of deep sea potential temperature drawn from the OSNAP is at Data access | OSNAP (o-snap.org) (Fu et al., 2023a, 2023b) and from the SAMOC at https://www.aoml.noaa.gov/phod/SAMOC_international/samoc_data.php (Meinen et al., 2018). The AMV index is available at https://psl.noaa.gov/data/timeseries/AMO (Enfield et al., 2001). Sea surface temperature data used in this study includes the ERSST data set version 5 at https://psl.noaa.gov/data/gridded/data.noaa.ersst.v5.html (Huang et al., 2017), the HadISST data set version 1 at https://www.metoffice.gov.uk/hadobs/hadisst/data/download.html (Rayner et al., 2003), and the BEST data set at https://berkeleyearth.org/data (Rohde & Hausfather, 2019). The ETOPO1 global relief model is at https://ngdc.noaa.gov/mgg/global/global.html.

Acknowledgments
This study is supported by National Natural Science Foundation of China Project (42130607), Laoshan Laboratory (LSKJ202202600), and National Key R&D Program of China (2023YFF0805100). We thank the help from Chris Atkinson and Simon Good, the principals of EN4 data set, for more details about the data set used in this study. And we acknowledge inspired discussions with Yingzhe Cui.

References

Antonov, J. I. (1993). Linear trends of temperature at intermediate and deep layers of the North-Atlantic and the North Pacific Oceans: 1957–1981. *Journal of Climate*, *6*(10), 1928–1942. https://doi.org/10.1175/1520-0442(1993)006<1928:Ltotai>2.0.Co;2

Ba, J., Keenlyside, N. S., Park, W., Latif, M., Hawkins, E., & Ding, H. (2013). A mechanism for Atlantic multidecadal variability in the Kiel Climate Model. *Climate Dynamics*, *41*(7–8), 2133–2144. https://doi.org/10.1007/s00382-012-1633-4

Chen, X. Y., & Tung, K. K. (2014). Varying planetary heat sink led to global-warming slowdown and acceleration. *Science*, *345*(6199), 897–903. https://doi.org/10.1126/science.1254937

Cunningham, S. A., Kanzow, T., Rayner, D., Baringer, M. O., Johns, W. E., Marotzke, J., et al. (2007). Temporal variability of the Atlantic meridional overturning circulation at 26.5 degrees N. *Science*, *317*(5840), 935–938. https://doi.org/10.1126/science.1141304

Davis, R. E. (1978). Predictability of sea level pressure anomalies over the North Pacific Ocean. *Journal of Physical Oceanography*, *8*(2), 233–246. https://doi.org/10.1175/1520-0485(1978)008<0233:Poslpa>2.0.Co;2

Delworth, T. L., & Mann, M. E. (2000). Observed and simulated multidecadal variability in the Northern Hemisphere. *Climate Dynamics*, *16*(9), 661–676. https://doi.org/10.1007/s003820000075

Dima, M., & Lohmann, G. (2010). Evidence for two distinct modes of large-scale ocean circulation changes over the last century. *Journal of Climate*, *23*(1), 5–16. https://doi.org/10.1175/2009jcli2867.1

Drijfhout, S., van Oldenborgh, G. J., & Cimatoribus, A. (2012). Is a decline of AMOC causing the warming hole above the North Atlantic in observed and modeled warming patterns? *Journal of Climate*, *25*(24), 8373–8379. https://doi.org/10.1175/Jcli-D-12-00490.1

Enfield, D. B., Mestas-Nunez, A. M., & Trimble, P. J. (2001). The Atlantic multidecadal oscillation and its relation to rainfall and river flows in the continental US. *Geophysical Research Letters*, *28*(10), 2077–2080. https://doi.org/10.1029/2000gl012745

Frajka-Williams, E., Meinen, C. S., Johns, W. E., Smeed, D. A., Duchez, A., Lawrence, A. J., et al. (2016). Compensation between meridional flow components of the Atlantic MOC at 26 degrees N. *Ocean Science*, *12*(2), 481–493. https://doi.org/10.5194/os-12-481-2016

Fu, Y., Lozier, M. S., Biló, T. C., Bower, A. S., Cunningham, S. A., Frédéric, C., et al. (2023a). Seasonality of the Meridional Overturning Circulation in the subpolar North Atlantic. *Communications Earth & Environment*, *4*(1), 181. https://doi.org/10.1038/s43247-023-00848-9

Fu, Y., Lozier, M. S., Biló, T. C., Bower, A. S., Cunningham, S. A., Frédéric, C., et al. (2023b). Meridional overturning circulation observed by the Overturning in the Subpolar North Atlantic Program (OSNAP) array from August 2014 to June 2020 [Dataset]. Georgia Institute of Technology. https://doi.org/10.35090/gatech/70342

Goldenberg, S. B., Landsea, C. W., Mestas-Nunez, A. M., & Gray, W. M. (2001). The recent increase in Atlantic hurricane activity: Causes and implications. *Science*, *293*(5529), 474–479. https://doi.org/10.1126/science.1060040

Good, S. A., Martin, M. J., & Rayner, N. A. (2013). EN4: Quality controlled ocean temperature and salinity profiles and monthly objective analyses with uncertainty estimates. *Journal of Geophysical Research-Oceans*, *118*(12), 6704–6716. https://doi.org/10.1002/2013jc009067

Gulev, S. K., Latif, M., Keenlyside, N., Park, W., & Koltermann, K. P. (2013). North Atlantic Ocean control on surface heat flux on multidecadal timescales. *Nature*, *499*(7459), 464–467. https://doi.org/10.1038/nature12268

Han, Z., Luo, F. F., & Wan, J. H. (2016). The observational influence of the North Atlantic SST tripole on the early spring atmospheric circulation. *Geophysical Research Letters*, *43*(6), 2998–3003. https://doi.org/10.1002/2016gl068099

Hayes, C. T., Costa, K. M., Anderson, R. F., Calvo, E., Chase, Z., Demina, L. L., et al. (2021). Global Ocean sediment composition and burial flux in the deep sea. *Global Biogeochemical Cycles*, *35*(4). e2020GB006769. https://doi.org/10.1029/2020GB006769

Hirschi, J. J. M., Barnier, B., Boning, C., Biastoch, A., Blaker, A. T., Coward, A., et al. (2020). The Atlantic meridional overturning circulation in high-resolution models. *Journal of Geophysical Research-Oceans*, *125*(4). e2019JC015522. https://doi.org/10.1029/2019JC015522

Huang, B., Thorne, P. W., Banzon, V. F., Boyer, T., Chepurin, G., Lawrimore, J. H., et al. (2017). NOAA Extended Reconstructed Sea Surface Temperature (ERSST), version 5 [Dataset]. NOAA National Centers for Environmental Information. https://doi.org/10.7289/V5T72FNM

Keenlyside, N. S., Latif, M., Jungclaus, J., Kornblueh, L., & Roeckner, E. (2008). Advancing decadal-scale climate prediction in the North Atlantic sector. *Nature*, *453*(7191), 84–88. https://doi.org/10.1038/nature06921

Kerr, R. A. (2000). A North Atlantic climate pacemaker for the centuries. *Science*, *288*(5473), 1984–1986. https://doi.org/10.1126/science.288.5473.1984

Kiss, A. E., Hogg, A. M., Hannah, N., Dias, F. B., Brassington, G. B., Chamberlain, M. A., et al. (2020). ACCESS-OM2 v1.0: A global ocean-sea ice model at three resolutions. *Geoscientific Model Development*, *13*(2), 401–442. https://doi.org/10.5194/gmd-13-401-2020

Knight, J. R., Allan, R. J., Folland, C. K., Vellinga, M., & Mann, M. E. (2005). A signature of persistent natural thermohaline circulation cycles in observed climate. *Geophysical Research Letters*, *32*(20), Article L20708. https://doi.org/10.1029/2005gl024233

Latif, M., Boning, C., Willebrand, J., Biastoch, A., Dengg, J., Keenlyside, N., et al. (2006). Is the thermohaline circulation changing? *Journal of Climate*, *19*(18), 4631–4637. https://doi.org/10.1175/jcli3876.1

Li, Q., England, M. H., Hogg, A. M., Rintoul, S. R., & Morrison, A. K. (2023). Abyssal ocean overturning slowdown and warming driven by Antarctic meltwater. *Nature*, *615*(7954), 841–847. https://doi.org/10.1038/s41586-023-05762-w

Li, Y., Li, J. P., & Feng, J. (2012). A teleconnection between the reduction of rainfall in southwest western Australia and North China. *Journal of Climate*, *25*(24), 8444–8461. https://doi.org/10.1175/jcli-d-11-00613.1

Liu, W., Xie, S. P., & Lu, J. (2016). Tracking ocean heat uptake during the surface warming hiatus. *Nature Communications*, *7*(1), 10926. https://doi.org/10.1038/ncomms10926

Marshall, J., & Speer, K. (2012). Closure of the meridional overturning circulation through Southern Ocean upwelling. *Nature Geoscience*, *5*(3), 171–180. https://doi.org/10.1038/ngeo1391

Mat, A. M., Sarrazin, J., Markov, G. V., Apremont, V., Dubreuil, C., Eche, C., et al. (2020). Biological rhythms in the deep-sea hydrothermal mussel Bathymodiolus azoricus. *Nature Communications*, *11*(1), 3454. https://doi.org/10.1038/s41467-020-17284-4

McCabe, G. J., Palecki, M. A., & Betancourt, J. L. (2004). Pacific and Atlantic Ocean influences on multidecadal drought frequency in the United States. *Proceedings of the National Academy of Sciences of the United States of America*, *101*(12), 4136–4141. https://doi.org/10.1073/pnas.0306738101

McCarthy, G. D., Brown, P. J., Flagg, C. N., Goni, G., Houpert, L., Hughes, C. W., et al. (2020). Sustainable observations of the AMOC: Methodology and technology. *Reviews of Geophysics*, *58*(1), e2019RG000654. https://doi.org/10.1029/2019RG000654

Meinen, C. S., Speich, S., Piola, A. R., Ansorge, I., Campos, E., Kersalé, M., et al. (2018). Meridional overturning circulation transport variability at 34.5°S during 2009–2017: Baroclinic and barotropic flows and the dueling influence of the boundaries. *Geophysical Research Letters*, *45*(9), 4180–4188. https://doi.org/10.1029/2018GL077408

Meng, M., & Gong, D. Y. (2022). Winter North Atlantic SST as a precursor of spring Eurasian wildfire. *Geophysical Research Letters*, *49*(18). e2022GL099920. https://doi.org/10.1029/2022GL099920

North, G. R., Bell, T. L., Cahalan, R. F., & Moeng, F. J. (1982). Sampling errors in the estimation of empirical orthogonal functions. *Monthly Weather Review*, *110*(7), 699–706. https://doi.org/10.1175/1520-0493(1982)110<0699:Seiteo>2.0.Co;2

Rayner, N. A., Parker, D. E., Horton, E. B., Folland, C. K., Alexander, L. V., Rowell, D. P., & Kaplan, A. (2003). Global analyses of sea surface temperature, sea ice, and night marine air temperature since the late nineteenth century. *Journal of Geophysical Research*, *108*(D14), 4407. https://doi.org/10.1029/2002JD002670

Rintoul, S. R. (1991). South-Atlantic interbasin exchange. *Journal of Geophysical Research*, *96*(C2), 2675–2692. https://doi.org/10.1029/90jc02422

Robson, J., Ortega, P., & Sutton, R. (2016). A reversal of climatic trends in the North Atlantic since 2005. *Nature Geoscience*, *9*(7), 513–517. https://doi.org/10.1038/Ngeo2727

Rohde, R., & Hausfather, Z. (2019). Berkeley Earth combined Land and Ocean temperature field, Jan 1850-Nov 2019 [Dataset]. Zenodo. https://doi.org/10.5281/zenodo.3634713

Rowell, D. P. (2003). The impact of Mediterranean SSTs on the Sahelian rainfall season. *Journal of Climate*, *16*(5), 849–862. https://doi.org/10.1175/1520-0442(2003)016<0849:Tiomso>2.0.Co;2

Smeed, D. A., Josey, S. A., Beaulieu, C., Johns, W. E., Moat, B. I., Frajka-Williams, E., et al. (2018). The North Atlantic Ocean is in a state of reduced overturning. *Geophysical Research Letters*, *45*(3), 1527–1533. https://doi.org/10.1002/2017gl076350

Sun, C., Li, J. P., Jin, F. F., & Ding, R. Q. (2013). Sea surface temperature inter-hemispheric dipole and its relation to tropical precipitation. *Environmental Research Letters*, *8*(4), Article 044006. https://doi.org/10.1088/1748-9326/8/4/044006

Sutton, R. T., McCarthy, G. D., Robson, J., Sinha, B., Archibald, A. T., & Gray, L. J. (2018). Atlantic multidecadal variability and the UK ACSIS program. *Bulletin of the American Meteorological Society*, *99*(2), 415–425. https://doi.org/10.1175/bams-d-16-0266.1

Trenberth, K. E., Fasullo, J. T., von Schuckmann, K., & Cheng, L. J. (2016). Insights into Earth's energy imbalance from multiple sources. *Journal of Climate*, *29*(20), 7495–7505. https://doi.org/10.1175/Jcli-D-16-0339.1

Tung, K. K., & Zhou, J. S. (2013). Using data to attribute episodes of warming and cooling in instrumental records. *Proceedings of the National Academy of Sciences of the United States of America*, *110*(6), 2058–2063. https://doi.org/10.1073/pnas.1212471110

Winton, M., & Sarachik, E. S. (1993). Thermohaline oscillations induced by strong steady salinity forcing of ocean general-circulation models. *Journal of Physical Oceanography*, *23*(7), 1389–1410. https://doi.org/10.1175/1520-0485(1993)023<1389:Toibss>2.0.Co;2

Yan, X. Q., Zhang, R., & Knutson, T. R. (2017). The role of Atlantic overturning circulation in the recent decline of Atlantic major hurricane frequency. *Nature Communications*, *8*(1), Article 1695. https://doi.org/10.1038/s41467-017-01377-8

Yang, Q., Dixon, T. H., Myers, P. G., Bonin, J., Chambers, D., Van den Broeke, M. R., et al. (2016). Recent increases in Arctic freshwater flux affects Labrador Sea convection and Atlantic overturning circulation. *Nature Communications*, *7*(1), 10525. https://doi.org/10.1038/ncomms13545

Zhang, R. (2008). Coherent surface-subsurface fingerprint of the Atlantic meridional overturning circulation. *Geophysical Research Letters*, *35*(20). https://doi.org/10.1029/2008gl035463

Zhang, R., Sutton, R., Danabasoglu, G., Kwon, Y. O., Marsh, R., Yeager, S. G., et al. (2019). A review of the role of the Atlantic meridional overturning circulation in Atlantic multidecadal variability and associated climate impacts. *Reviews of Geophysics*, *57*(2), 316–375. https://doi.org/10.1029/2019rg000644